Device dependent distortion correction in time-stretch photonic analog to digital converters using deep neural networks

Mandeep Singh, Joydip Dutta, Sreeraj S J, Viswanathan Sankar, Balaji Srinivasan, Lakshmi Narasimhan Theagarajan, and Deepa Venkitesh*

Department of Electrical Engineering, Indian Institute of Technology Madras, Chennai, India

**deepa@ee.iitm.ac.in*

Abstract: We experimentally demonstrate a novel deep learning-aided time-stretch photonic front end architecture to overcome device-dependent distortions to improve the signal-to-noise and distortion ratio by more than 24 dB, and reduce the bandwidth requirements of the back-end electronic ADC by three times.

1. Introduction

Increase in data rates in both RF and optical communication systems demand the need for better analog to digital converters (ADCs), that keeps up with the bandwidth and effective number of bit (ENOB) requirements. Improvement in spectral efficiency in optical communication would require scaling of constellations from 16 to 64QAM and higher, and such scaling is ultimately limited by the ENOB at the receiver. The ENOB degradation is primarily contributed by the timing jitter of the sampling clock. The ENOB is theoretically limited to about 4.2, when 100 GHz bandwidth signal is sampled by an electronic clock with a timing jitter of 67 fs [1].

Time Stretch Photonic Analog to Digital Converters (TS-PADCs) allow high bandwidth signal acquisition with improved ENOB by time-to-wavelength mapping using photonic techniques. The high-frequency RF signals are converted to an equivalent, parallel low-frequency signals by modulating them onto a spectral rich optical pulsed source and then stretching it in the optical domain using a linear dispersive medium. The stretched signals are split to parallel channels using optical filters, which are further sampled using the electronic ADCs (eADCs). The time stretching process reduces the bandwidth requirement of the back-end eADC by the same factor as the Stretch Factor (SF) of the optical pulse. There have been demonstrations of TS-PADC in the past with its versions to improve its performance in terms of bit resolution and dynamic range such as single side band modulation [2, 3], differential-arcsine algorithm [4,5] and digital broadband linearization algorithm [6]. The key sources of distortion in a TS-PADC is the inefficient pulse envelope correction and the cross talk between the parallel channels due to the non-ideal nature of the wavelength filters. A redundancy detection method to mitigate these distortions was suggested in [7], but at the expense of additional hardware and complexity.

In this work, we carry out such device dependent distortion correction for continuous TS-PADCs using a deep learning framework for the first time to the best of our knowledge. Here, we consider distorted data sequences for different ranges of known input frequencies to train a simple Feed Forward Neural Network (FFNN). The trained model is tested on the live experimental system for a range of frequencies and signal power levels. An improvement of 24.4 dB in Signal-to-Noise and Distortion Ratio (SNDR) is observed for a TS-PADC with a stretch factor of 3.132 with the use of trained model.

2. Experimental Setup

The schematic of the continuous TS-PADC architecture to compensate device-dependent distortions using FFNN is shown in Fig.1(a). A spectrum-rich Mode-Locked Laser (MLL, pulse width : 200 fs, rep rate: 50 MHz) is used as the optical carrier, and is first stretched using a dispersive medium (D1, net dispersion of $\sim$ 595 ps/nm). These stretched pulses are fed to a bias-controlled dual-output Electro Optic Modulator (EOM) through the Polarization Controller (PC), where the analog RF signals are modulated on the stretched pulses. The complementary outputs of the EOM are time-interleaved using a delay line and combined using a 50:50 coupler, which is further used for shape-corrections. The modulated signal is further stretched using a second dispersive medium (D2, net dispersion of $\sim$1223 ps/nm), thus yielding an overall SF of 3.132. The stretched signal is then split using a 1×4 splitter, and four custom-designed band-pass filters are used to segregate the different spectral components. The spectra at the output of the 1×4 splitter and four filters are shown in the inset of Fig.1(a). The de-multiplexed outputs are fed to a four-channel photo detector (PD, bandwidth : 500 MHz) that converts the optical to electrical signals, followed by transimpedance amplifiers. Optical amplifiers are included in the path to maintain the power falling on the photo detector to be identical in all the four channels. The received analog signals are fed to a four-channel low-bandwidth ADC (bandwidth: 500 MHz, sampling rate: 1 GS/s), which is triggered using the reference electrical

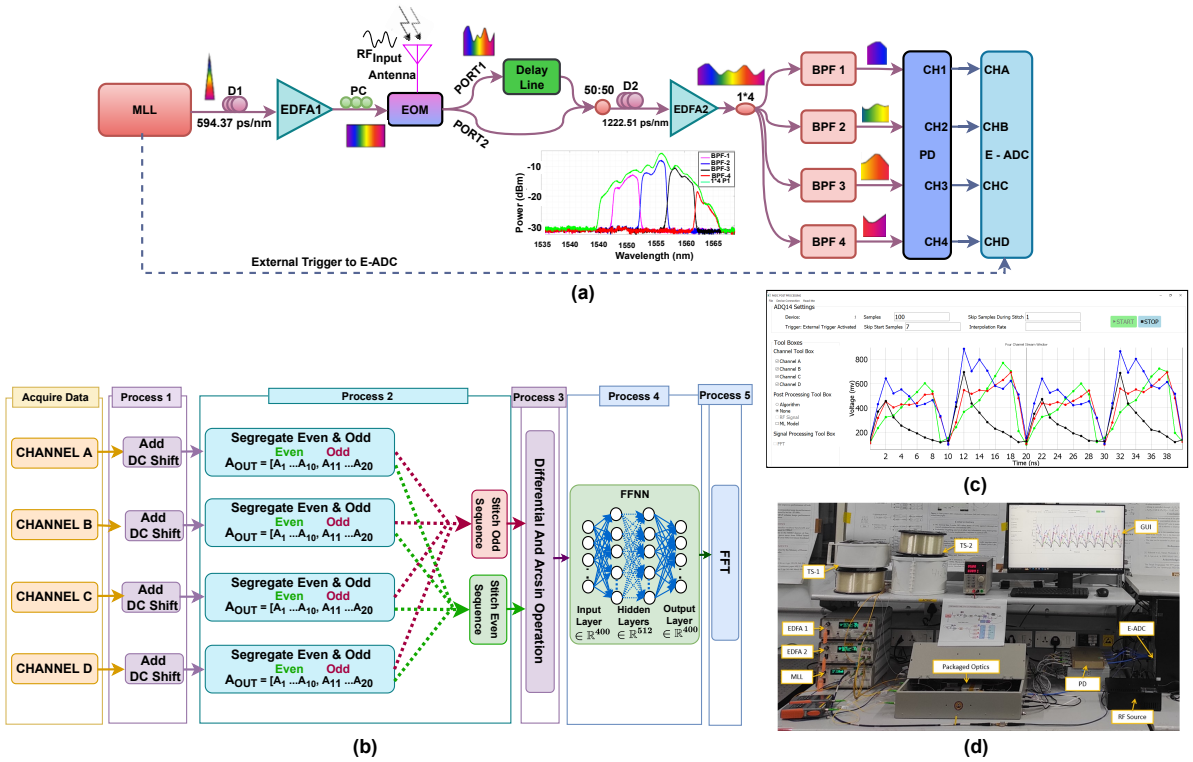

Fig. 1. (a) Schematic of the continuous TS-PADC architecture (b) post processing algorithm (c) customized graphical user interface (d) photograph of the experimental setup.

output of the MLL. The ADCs are mounted on a Kintex7 FPGA and further connected to a workstation. Digitized data is sent in real-time to the FIFO on the FPGA, transferred to the PC, and processed in the workstation. Fig.1(b) shows the post-processing steps, which include adding appropriate DC shift, de-interleaving the pulses in each channel corresponding to the two complementary ports of the modulator (into even and odd data sequences), stitching the four time domain data corresponding to the four channels in both even and odd data sequences, and then performing differential and arcsin operation to generate a continuous-time domain waveform of the expected RF, whose frequency is scaled down with respect to the input frequency by the SF. The differential and arcsin operation is carried out to compensate for the pulse-shape induced distortions. Further, to mitigate the device-dependent nonlinear distortions, the recovered data is fed to a trained FFNN model, to correct for all device-dependent distortions. The photograph of the customized graphical user interface and experimental setup is shown in Fig.1(c) and (d).

3. Experimental Results and Discussions

Figs. 2(a) and (b) show the time and frequency domain output in a red color corresponding to the raw data from an experiment where an input frequency of 1.61 GHz, 14 dBm is fed to the system. The recovered RF is expected to be scaled down by the SF and is expected at 370.3 MHz. However, from Fig 2(b), it is noticed that the recovered RF (shown in red) is observed as two peaks around 370.3 MHz with -1.68 dBm power. This offset/error is due to the stitching errors between adjacent channels, the 50 MHz repetition rate of the MLL, and other system distortions.

To mitigate these device-dependent nonlinear distortions, the FFNN is trained with time-series data obtained from the experiment. RF frequencies are varied from 0.61 GHz to 1.40 GHz with a step size of 5.1 MHz, and time domain data is captured. The dataset is further divided into two subsets: 75% for training the model and 25% for validation. The network training is implemented in PyTorch, with the maximum number of epochs set to 5000. The training data is sequentially processed by each hidden layer, and the output generated is solely determined by the input and the network parameters. After an extensive hyperparameter search, the architecture of the FFNN is chosen to have 4 layers having 400, 512, 512, and 400 nodes respectively with ReLU and Tanh as activation for hidden layers, and output layer respectively. Adam optimizer with a learning rate of 0.001 is deployed. To estimate real-valued RF frequencies, Mean Square Error (MSE) is employed as the loss function which is shown in Fig.2(c). It is observed that the training and validation losses decrease as the number of epochs increases, indicating the model's improving performance with training iterations.

To estimate the performance of the trained FFNN, the untrained RF data of 14 dBm at 1.16 GHz is fed to the

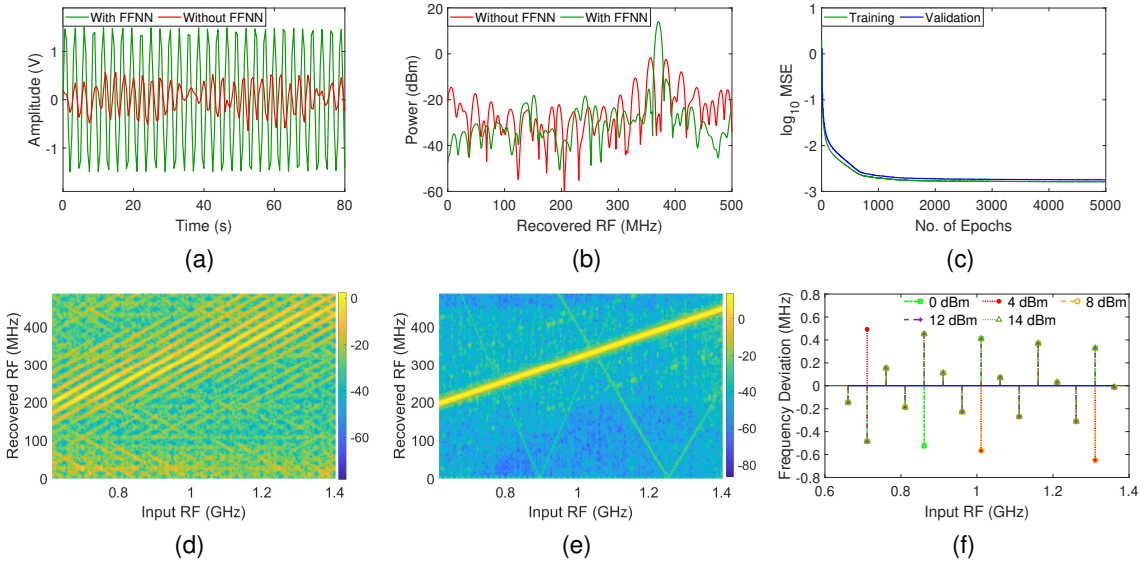

Fig. 2. (a) Time domain output for 1.16 GHz input, with (green) and without (red) FFNN (b) spectrum of the recovered RF with and without FFNN (c) convergence of FFNN model; recovered RF vs input RF (d) without FFNN model (e) with FFNN model (f) frequency deviation vs input RF with FFFN model at different RF power levels

trained model for predictions. It is observed from Figs. 2(a) and (b) (green color) that with the FFNN model, the recovered RF is observed at 370.3 MHz without an offset and all the distortions arising due to the stitching errors and amplitudes of the spurious tones are reduced significantly. The recovered RF tone is approximately at 14 dBm and the SNDR is approximately 25 dB, which can be computed using the following relation: SNDR $=$ $10\ \log_{10}(P_{Signal}/(P_{Noise}+P_{Distrortions}))$. The SNDR can be further improved with a pre-amplifier at the input of the EOM. It's important to note that the dynamic range of the proposed system is limited by the link design. Moreover, in order to confirm the system's performance across a wide spectrum of input RF signals spanning from 0.6 GHz to 1.4 GHz with a 5 MHz step, these frequencies are fed to the trained model in a completely independent experiment. The pseudocolor plots illustrating the recovered RFs, both with and without FFNN, for various input RF frequencies, are presented in Figs.2(d) and (e). The pseudocolor plot spectra without FFNN reveal that multiple RF peaks appear at lower power levels with frequency offsets, making it very difficult to distinguish the desired RF signals. However, with the trained FFNN model, a clean spectra is observed, with all distortions corrected. The the deviation in the recovered RF for different input RF is shown in Fig.2(f), where largest deviation in the recovered RF is < 0.75 MHz, which is within the 5 MHz frequency resolution of the system. This indicates the reliability of the fully connected trained FFNN model which can significantly improve the performance of the TS-PADC by minimizing the device-dependent distortions.

4. Conclusion

We have experimentally demonstrated detection of frequencies up to 1.61 GHz using electronic ADCs with a sampling rate of 1 GSa/s, through photonic time-stretching (stretch factor 3.13). We use a feed forward neural network (FFNN) to compensate for the device-dependent distortions and use the trained network in the live experiment to recover a broad range of frequencies with a frequency error < 0.6 MHz, resolution of 5 MHz, and with an improvement in SNDR of > 24 dB with the FFNN. Even though this specific demonstration is for sinusoids, the network can be trained for the digital, LFM modulated data for specific applications. The design is not bandwidth restrictive. The demonstration provides a novel pathway to enable accurate digitisation of high-frequency and wideband signals in ultra-wide band radars, imaging and high capacity optical communication systems.

References

1. B. Murmann. [Online]. Available:https://github.com/bmurmann/ADC-survey.
2. Y. Han and B. Jalali, J. Light. Technol. **21**, 3085–3103 (2003).
3. Y. Han, O. Boyraz, and B. Jalali, IEEE Trans. on Microw. Theory Tech. **53**, 1404–1408 (2005).
4. S. Gupta, G. C. Valley, and B. Jalali, J. Light. Technol. **25**, 3716–3721 (2007).
5. S. Gupta and B. Jalali, Opt. Lett. **33**, 2674–2676 (2008).
6. A. Fard, S. Gupta, and B. Jalali, Opt. Lett. **36**, 1077–1079 (2011).
7. S. Yang, J. Wang, H. Chi, and B. Yang, Appl. Opt. **60**, 1646–1652 (2021).